Bioresource Technology Reports 3 (2018) 75–81

Contents lists available at ScienceDirect

Bioresource Technology Reports

journal homepage: www.journals.elsevier.com/bioresource-technology-reports

Performance of novel biosorbents prepared using native and NaOH treated *Peltophorum pterocarpum* fruit shells for the removal of malachite green

S. Rangabhashiyam[a,*], P. Balasubramanian[b,*]

[a] Department of Biotechnology, School of Chemical and Biotechnology, SASTRA University, Thanjavur 613401, Tamilnadu, India
[b] Department of Biotechnology and Medical Engineering, National Institute of Technology Rourkela, Odisha 769 008, India

ARTICLE INFO

Keywords:
Peltophorum pterocarpum fruit shells
Modification
Malachite green

ABSTRACT

The *Peltophorum pterocarpum* fruit shells were treated with sodium hydroxide, employed for the malachite green biosorption. Biosorbents characterization conducted using the Environmental Scanning Electron Microscopy and X-ray Diffractometer. The MG removal performance was evaluated in a batch biosorption system by varying the process parameters. The biosorption data modeled using the Langmuir, Freundlich, Tempkin, Halsey and Jovanovic isotherm models. The Langmuir model superior explained the equilibrium data among the isotherms considered in the current investigation. The maximum uptake capacity of 62.50 mg/g was observed for sodium hydroxide treated biomass, whereas native biosorbent showed 40.00 mg/g. The kinetic modeling of the experimental data revealed that the better fit of the pseudo-second-order kinetic model and suggested the mechanism of chemisorption. MG biosorption using sodium hydroxide treated biomass of enthalpy with positive values indicates endothermic and Gibbs free energy of negative values represented spontaneous nature.

1. Introduction

The fast growth industrialization in different sectors during the recent decades imposed harmful effects on the ecosystem. The wastewater generated from industries are associated with harmful substances of synthetic organic dyes, heavy metals, pharmaceuticals, complex organic compounds, etc. (Ebrahim et al., 2018; Piccirillo et al., 2017). The wastewater contaminant category of synthetic dyes correspond as an important contaminant and the effluent in the colored form are repeatedly discharged from the resultant of industrial activities such as textile, leather tanning, pulp mills, cosmetics, hair coloring and dye production, respectively (Farnaz et al., 2016; Rangabhashiyam et al., 2013). Adsorption of toxic dye by means of activated carbon reported with higher adsorption efficiency and widely employed for the treatment of harmful dyes sourced from different industrial effluent streams. Nevertheless, commercial usage of activated carbon constrained due to the more price and regeneration difficulty (Mustafa et al., 2014).

The sources of natural materials from industrial waste/by-product and biomass residues were used as the low cost biosorbents for the dyes biosorption. The waste biomass materials utilized for the biosorbent preparation presents the benefits of eco-friendliness, low cost, wide availability, biomass regeneration and dye recovery (Anna, 2011; Rangabhashiyam and Balasubramanian, 2018a). Recently, there is a mounting attention in the usage of plant based biomass residues as biosorbents, such as *Hymenaea courbaril* fruit shell (Isis et al., 2017), *Eichhornia crassipes* (Tapas and Naba, 2017), *Caryota urens* inflorescence (Rangabhashiyam and Selvaraju, 2015), *Aegle marmelos* leaves (Baruah et al., 2017), *Swietenia mahagoni* fruit shell (Rangabhashiyam et al., 2014a), *Metroxylon* sp. (Jeminat et al., 2016), *Luffa cylindrica* fibers (Aida et al., 2016), etc. Most of the reported biosorbents showed lower dye removal performance in its native form, therefore the biomass requires some pre-treatment in such a way to get better uptake capacity. The chemical procedure of biomass pre-treatment alters the biosorbent surface characteristic by presenting more dye interaction sites (Rangabhashiyam and Balasubramanian, 2018b). The alkali method modification of biomass by means of sodium hydroxide (NaOH) illustrated improved uptake capacity by the biosorbents. The use of NaOH as the modifying chemical agent involves the solubilization of some lignin fractions and other soluble organics in the biomass, allows the access of NaOH into the biomass matrix. The pre-treatment of biomass with sodium hydroxide augments the surface roughness, porosity, enhanced occurrence of hydroxyl and other reactive groups on the surface of biosorbent (Muhammad et al., 2015; Jain and Gogate, 2017).

In the current research, fruit shells of *Peltophorum pterocarpum* tested for the biosorption of malachite green. For this purpose, *Peltophorum pterocarpum* fruit shells were used as such i.e. native biomass and pre-treated with NaOH. The biosorption parameters were examined in the batch mode technique. Further, the analysis of

* Corresponding authors.
E-mail addresses: rambhashiyam@gmail.com (R. S.), biobala@nitrkl.ac.in (B. P.).

https://doi.org/10.1016/j.biteb.2018.06.004
Received 31 May 2018; Received in revised form 15 June 2018; Accepted 17 June 2018
Available online 07 July 2018
2589-014X/ © 2018 Elsevier Ltd. All rights reserved.

experimental data using the biosorption isotherm model and kinetic model were performed. The experimental data of the temperature parameter used for the thermodynamic parameter evaluation.

2. Materials and methods

2.1. Materials

The malachite green (MG) used as a model pollutant in the present experiment. The MG stock solutions concentration of 1000 mg/L was prepared. The desired concentrations of working solutions were prepared through the dilutions of the stock solution. Distilled water subjected for the solutions preparations throughout the study. Diluted NaOH and/or HCl used to regulate the pH of the solution. The model pollutant MG used in the current investigation with no additional purification. The entire chemical reagents employed for the biosorption were of analytical grades. The important properties of the biosorbents were determined using pertinent techniques of Field Emission Scanning Electron Microscopy (FE-SEM) (Quanta 250 FEG) and X-ray diffraction (XRD) (Rigaku Ultima-IV) analyzer.

2.2. Preparation of biosorbents

The fruit shells of *Peltophorum pterocarpum* was collected in Rourkela, India. The collected biomass first washed using water to remove the dust and subsequently washed using distilled water. The dirt free biomass dried in hot air oven at 333 K for 24 h. Then the biomass was grinded, put through a sieve for getting the biomass 0.1 mm–0.2 mm, size. A portion of the prepared biomass employed in the native form (PFS) for MG biosorption. Another portion of the biomass used for the preparation of modified biosorbent using NaOH pretreatment (SPFS). The prepared biomass suspended in 500 mL of 0.1 M NaOH and agitated for 24 h at room temperature. The modified biomass was separated from the mixture through filtration process and then washed by distilled water in such a way to eliminate the presence of any excess NaOH followed by the drying in oven at 383 K for 2 h. The resultant PFS and SPFS tested for the MG biosorption experiments.

2.3. Experimental methodology

In the batch system, a standard biosorption procedure consisting of exact amount of biosorbent contacted to a fixed volume of MG solution under controlled conditions of process parameter such as initial solution pH, agitation speed and temperature. The 50 mL of MG solution (Initial concentration, 20–100 mg/L) was transferred into conical flasks and the content stirred at 120 rpm. The dosage of PFS, SPFS studied from 0.02 g to 0.18 g and the initial solution pH varied from 2.0 to 10.0. The temperature effect on the MG removal process was performed at different temperatures. The MG concentrations in aqueous solutions were analyzed by absorbance measurement of the solutions at 619 nm using UV–visible spectrophotometer (Systronics 2203).

The MG uptake at equilibrium time q_e (mg/g) was determined through the given expression:

$$q_e = \frac{(C_0 - C_e)}{m} \times V_L \tag{1}$$

The percentage removal of MG was determined as follows:

$$Removal\,(\%) = \frac{(C_0 - C_e)}{C_0} \times 100 \tag{2}$$

C_0 the original MG concentration (mg/L) and C_e the concentration of MG at equilibrium (mg/L), m is the dosage of biosorbent (g) and V_L total volume (L).

2.4. Biosorption isotherm models

The isotherms are important to depict the interaction between biosorbent and biosorbate, associated mechanisms and prediction of biosorption capacity. The establishments of the most suitable correlation for the equilibrium studies are essential. There are different isotherm models are available to demonstrate the equilibrium nature of the biosorption process (Rangabhashiyam et al., 2014b). The batch experiment data were processed using Langmuir, Freundlich, Tempkin, Halsey and Jovanovic models.

The Langmuir model considers the assumptions that no interaction occurs between the biosorbed species. The isotherm characterizes the distribution of MG between the solution and biosorbent solid phase. This model finds application in evaluating the highest uptake capacities (Langmuir, 1918). The model indicated as follows:

$$\frac{C_e}{q_e} = \frac{1}{K_L q_m} + \frac{C_e}{q_m} \tag{3}$$

where q_m the maximum uptake capacity (mg/g) and K_L the Langmuir constant (L/mg).

The Freundlich model represents empirical equation, appropriate to multilayer or heterogeneous surfaces (Freundlich and Helle, 1939). The Freundlich model has the following form:

$$\log q_e = \log K_F + \frac{1}{n_F} \log C_e \tag{4}$$

K_F Freundlich isotherm constant and n_F denote biosorption intensity, used to indicate favorability of the biosorption process. According to the Freundlich model, the favorable biosorption process will occur for the value of $1 / n_F$ between 0 and 1.

The Tempkin model comprehends the effect of biosorbent–biosorbate interactions. The model considers the assumption that because of biosorbate–biosorbate repulsions the heat of biosorption of all layer molecules reduces linearly with the molecules coverage and the biosorbate biosorption uniformly distributed (Tempkin and Pyzhev, 1940). The Tempkin model mentioned in the following form:

$$q_e = \left(\frac{RT}{b_T}\right) \ln A_T + \left(\frac{RT}{b_T}\right) \ln C_e \tag{5}$$

where R the universal gas constant (8.314 J/mol K), T the absolute temperature (K), b_T constant connected to the heat of biosorption and A_T the Tempkin model constant (L/mg).

The Halsey isotherm model provides description on the condensation of multilayer process at a comparatively higher distance from the surface. The model indicates the distribution of heterogeneous pore nature of the biosorbent (Halsey, 1948). The Halsey model given as follows:

$$\ln q_e = \frac{1}{n_H} \ln K_H - \frac{1}{n_H} \ln \frac{1}{C_e} \tag{6}$$

where K_H represent Halsey isotherm constant and n_H indicate exponent of Halsey isotherm model.

The Jovanovic isotherm model considers the likelihood of mechanical contacts occurrence among the biosorbing and desorbing biosorbate on the uniform surface. The assumptions of the Jovanovic isotherm model are same to that of the assumptions used in the Langmuir model (Jovanovic, 1969). The Jovanovic model indicated in the following form:

$$\ln q_e = \ln Q_m - K_J C_e \tag{7}$$

where Q_m the maximum biosorption capacity (mg/g) and K_J Jovanovic isotherm constant (L/g).

2.5. Biosorption kinetic models

The biosorption equilibrium relationships comprise of different

operating conditions, and the time required for the biosorption to attain thermodynamic stable. The biosorption rate mainly based on the leading way starting from the initial stage of biosorption process until the equilibrium final state. The different mechanisms associated with the biosorption process include mass transfer, chemical reactions and particle diffusion control (Ho et al., 2000). The controlling mechanism of MG uptake using PFS and SPFS was examined by fitting the experimental biosorption data to pseudo-first-order, pseudo-second-order and intra-particle diffusion kinetic models.

The pseudo-first-order kinetic model considers the assumption that the rate of interaction limited with only one of the process otherwise the mechanism on a particular type of biosorption sites dependent on time. The Lagergren kinetic model applicable only during the early stage of the biosorption process (Lagergren, 1898). The pseudo-first-order kinetic model represented by:

$$\log(q_e - q_t) = \log q_e - \frac{k_1}{2.303} t \quad (8)$$

where k_1 the pseudo-first-order rate constant of the biosorption process (1/min), q_e and q_t the amount of MG biosorbed (mg/g) at equilibrium and at time t (min), respectively.

The pseudo-second-order kinetic model assumes that the chemisorption as the rate-limiting step. The important mechanisms governed in the biosorption process are ion-exchange, complexation and depends on the biosorbent uptake capacity (Ho and McKay, 1999). The pseudo-second-order equation written in the following form:

$$\frac{t}{q_t} = \frac{1}{k_2 q_e^2} + \frac{t}{q_e} \quad (9)$$

where k_2 the rate constant of pseudo-second-order kinetic model (g/mg min).

The biosorption involves the solute transport from bulk solution to the interior pores surface of the biosorbent and this step becomes the rate-controlling factor in some biosorption process. The intra-particle diffusion model proposed by Weber and Morris used to investigate the diffusion controlled biosorption system (Weber and Morris, 1962). The intra-particle diffusion model expressed as follows:

$$q_t = k_{id} t^{1/2} + C \quad (10)$$

k_{id} the intra-particle diffusion rate constant (mg/g $\text{min}^{1/2}$) and C the intercept, which gives information on boundary layer thickness.

2.6. Thermodynamics

The characteristics of biosorbent on the dye removal process expressed through the evaluation of thermodynamic parameters, which offers insights into mechanisms of the biosorption. Thermodynamics parameters were calculated using the following equation:

$$\ln K_C = \frac{-\Delta H^\circ}{RT} + \frac{\Delta S^\circ}{R} \quad (11)$$

$$\Delta G^\circ = -RT \ln K_C \quad (12)$$

where K_c the distribution coefficient of MG between aqueous solution and solid phase of the biosorbent.

3. Results and discussion

3.1. Characterization of the biosorbents

SEM analysis is a potential tool for characterization of the surface morphology of biosorbents. The SEM images clearly present the surface texture of the biosorbents of native and sodium hydroxide treated forms. There observed significant changes in the surface morphology of the sodium hydroxide treated biosorbent. The PFS consists of rough grooves surface without occurrence of major cracks or cavities. The SEM image of SPFS showed the presence of porous, irregular and high heterogeneity compared to PFS. The distribution of porous structure in SPFS might offer good dye accessibility, functional group interactions and promote biosorption of MG molecules. The XRD pattern of PFS showed the presence of characteristic peaks at 2θ values of 22.14°, 24.33° and 34.68° respectively. For SPFS, the XRD peaks obtained at 2θ values of 21.63°, 24.30° and 34.52° respectively. The XRD patterns of both the biosorbents PFS and SPFS denoted the highly ordered crystal regions of cellulose (Malvin et al., 2017), which are involved in MG biosorption.

Table 1
The thermodynamic parameters for biosorption of MG onto PFS and SPFS.

C_0 (mg/L)	T (K)	PFS			SPFS		
		ΔG° (kJ/mol)	ΔH° (kJ/mol)	ΔS° (J/mol K)	ΔG° (kJ/mol)	ΔH° (kJ/mol)	ΔS° (J/mol K)
20	303	−5.49	−24.40	−62.05	−7.79	3.38	36.90
	313	−5.08			−8.17		
	323	−4.49			−8.55		
	333	−3.60			−8.89		
40	303	−4.23	−22.81	−61.29	−6.89	7.25	46.59
	313	−3.65			−7.33		
	323	−2.97			−7.71		
	333	−2.42			−8.32		
60	303	−3.19	−17.42	−46.61	−5.19	18.33	77.76
	313	−2.94			−6.05		
	323	−2.53			−6.80		
	333	−1.75			−7.53		
80	303	−2.27	−17.35	−50.00	−4.03	23.37	90.53
	313	−1.52			−4.91		
	323	−1.30			−6.04		
	333	−0.69			−6.66		
100	303	−1.27	−11.00	−32.04	−3.33	21.40	81.26
	313	−1.01			−3.82		
	323	−0.62			−4.87		
	333	−0.33			−5.70		

Table 2
The isotherm parameters for biosorption of MG onto PFS and SPFS.

Isotherm model	Biosorbent	
	PFS	SPFS
Langmuir		
q_m	40.00	62.50
K_L	0.2314	0.3636
R^2	0.995	0.986
Freundlich		
K_F	8.91	17.37
n_F	2.1505	2.2779
R^2	0.985	0.978
Tempkin		
b_T	0.3044	0.2048
A_T	1.0000	1.0015
R^2	0.991	0.988
Halsey		
K_H	0.0090	0.0014
n_H	−2.1505	−2.2779
R^2	0.985	0.978
Jovanovic		
Q_m	11.27	17.51
K_J	−0.063	−0.090
R^2	0.740	0.762

3.2. Effect of pH

The removal of MG using PFS and SPFS was studied in the solution pH range of 2.0–10.0 with an initial MG concentration of 20 mg/L. The

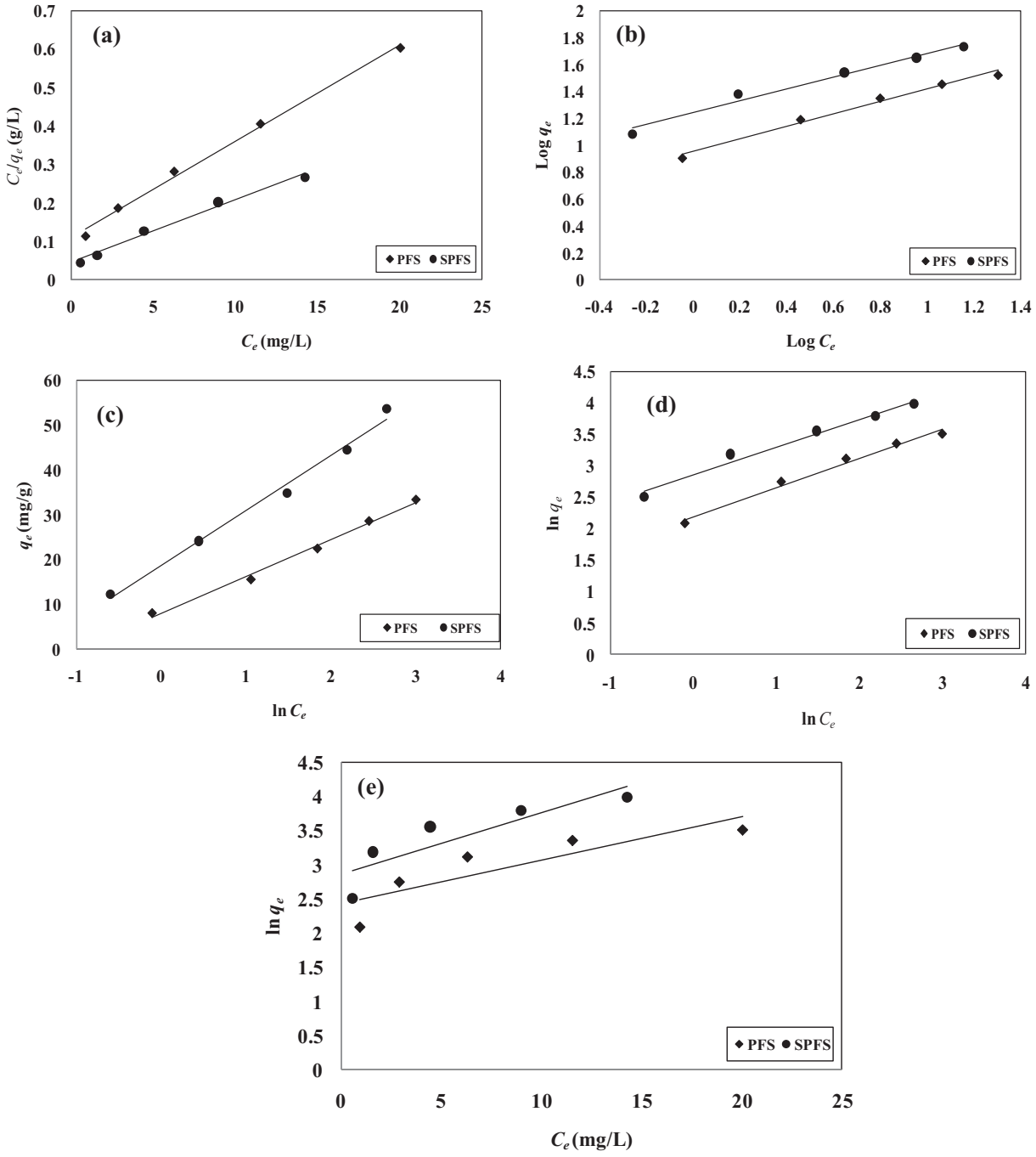

Fig. 1. Isotherms plots of (a) Langmuir, (b) Freundlich, (c) Tempkin, (d) Halsey and (e) Jovanovic, for the biosorption of MG using PFS and SPFS.

results showed the gradual increase of MG removal up to pH 10.0 and pH 8.0 for PFS and SPFS. The maximum biosorption capacity were recorded as 7.94 (PFS) and 12.15 mg/g (SPFS) at pH 10.0 (PFS) and 8.0 (SPFS) respectively. Whereas, the maximum values of removal efficiency were 95.38% (PFS) at pH 10.0 and 97.24% (SPFS) at pH 8.0.

The initial pH is one of the main parameter in the MG removal process, since it influences on the biosorbent surface charge and degree of ionisation of the biosorbate molecules. The removal of MG by PFS and SPFS showed lower removal performance at the pH range from 2.0 to 7.0. The more number of positively charged surface sites on the biosorbent at the acidic pH range affects the binding of positively charged MG dye molecules through electrostatic repulsion and excess H^+ ions compete with MG for the biosorption sites on PFS and SPFS (Mohd and Rasyidah, 2011). Similar results were reported for the biosorption of MG using *Citrus limetta* Peel and *Zea mays* Cob (Hemant et al., 2017). The optimized initial pH of 10.0 (PFS) and 8.0 (SPFS) was fixed for the entire biosorption experiments.

3.3. Effect of biosorbents dosage

To investigate the effect of PFS and SPFS dosage on MG biosorption, experiments were conducted at initial MG concentration of 20 mg/L and the amount of biosorbents varied in the range of 0.02–0.18 g. The process parameter of biosorbent dosage determines the removal ability of biosorbate by the biosorbent. The percentage of MG removal increased from 85.20% to 95.50% (PFS) and from 90.95% to 97.24% (SPFS), for the dosage raise from 0.02 g to 0.12 g (PFS) and from 0.02 g to 0.08 g (SPFS), respectively. The higher biosorbent dosage offers more

Table 3
The kinetic parameters for biosorption of MG onto PFS and SPFS.

Kinetic model	Biosorbent	Malachite green (mg/L)				
		20	40	60	80	100
Pseudo-first-order						
k_1 (1/min)	PFS	0.0322	0.0345	0.0253	0.0345	0.0414
q_e (mg/g)		2.60	5.49	8.39	13.03	18.66
R^2		0.812	0.864	0.805	0.915	0.954
k_1 (1/min)	SPFS	0.0437	0.0414	0.0322	0.0345	0.0345
q_e (mg/g)		5.61	11.93	13.61	18.66	26.54
R^2		0.910	0.867	0.853	0.847	0.850
Pseudo-second-order						
k_2 (g/mg min)	PFS	0.0399	0.0192	0.0092	0.0064	0.0048
q_e (mg/g)		8.13	15.87	23.25	30.30	35.71
R^2		0.999	0.999	0.998	0.999	0.999
k_2 (g/mg min)	SPFS	0.0266	0.0095	0.0068	0.0050	0.0033
q_e (mg/g)		12.50	25.00	35.71	45.45	55.55
R^2		0.999	0.999	0.999	0.998	0.997
Intra-particle diffusion						
k_{id} (mg/g min$^{1/2}$)	PFS	0.141	0.322	0.537	0.799	1.049
C (mg/g)		6.45	12.17	16.48	20.26	22.65
R^2		0.966	0.914	0.984	0.950	0.962
k_{id} (mg/g min$^{1/2}$)	SPFS	0.254	0.539	0.738	0.973	1.436
C (mg/g)		9.55	18.37	26.79	33.87	38.07
R^2		0.970	0.983	0.994	0.994	0.975

number of biosorption sites at the surface of the biosorbent, resultant to the increased MG removal efficiency by the biosorbent from the aqueous medium. Nevertheless, the uptake capacity of PFS and SPFS illustrated declined outcome for the raise of biosorbent dosage. The results are due to the overlapping of biosorption sites or biosorbents aggregation, which limits the number of available biosorption sites stoichiometrically (Rangabhashiyam et al., 2018). The optimal biosorbent dosage of 0.12 g (PFS) and 0.08 g (SPFS) selected for the biosorption experiments.

3.4. Effect of initial MG concentration

To investigate the influence of initial MG concentration on the biosorption process, the initial MG concentration varied from 20 to 100 mg/L. For the increase of initial MG concentration, the removal efficiency of PFS and SPFS showed decreased performance of 95.50% to 79.94% and 97.24% to 85.74%. The percentage removal of MG was observed higher at lower initial MG concentration and smaller at higher MG initial concentration. Whereas, the biosorption capacity of PFS and SPFS was found increased with the increase of initial MG concentration from 20 mg/L to 100 mg/L. The biosorption capacity of PFS towards MG, raised from 7.95 mg/g to 33.30 mg/g and using SPFS the biosorption capacity increased from 12.15 mg/g to 53.59 mg/g. The initial concentration of MG provides significant driving force for the diffusion of dyes from the aqueous solution onto biosorbents. The higher initial dye concentration of 100 mg/L, PFS showed higher uptake capacity compared to SPFS. A similar result was observed for the biosorption of MG from aqueous medium using sodium carbonate treated rice husk (Binod and Upendra, 2015).

3.5. Effect of temperature and thermodynamic study

The biosorption of MG onto PFS and SPFS was studied with varying initial MG concentrations and varying temperature of 303, 313, 323 and 333 K respectively. The experimental results of the biosorption of MG using PFS showed that the removal performance decreased with temperature increase for the initial MG concentration of 20–100 mg/L. In case of SPFS subjected biosorption process under temperature increase from 303 to 333 K, the performance towards MG removal found increased for all the studied initial MG concentration.

The thermodynamic results obtained for PFS and SPFS towards MG removal are shown in Table 1. The negative values for ΔG° observed in both PFS and SPFS for all the studied initial MG concentrations at different temperatures (Table 1). The results revealed that the biosorption process as thermodynamically feasible and spontaneous in nature (Rangabhashiyam et al., 2016). The increase in ΔG° values of SPFS for the temperature raise from 303 K to 333 K showed increase in biosorption feasibility. Nevertheless, for PFS the values of ΔG° decreased for the temperature increase denoted non-spontaneous nature of biosorption process. The ΔH° values (-24.40, -22.81, -17.42, -17.35 and -11.00 kJ/mol) for the biosorption of all the studied MG using PFS observed negative suggests exothermic process. The positive values of ΔH° (3.38, 7.25, 18.33, 23.37 and 21.40 kJ/mol) demonstrated that the interaction of all studied concentration of MG on SPFS as endothermic in nature and the results are supported with the increased MG biosorption at higher temperature. The negative values of ΔS° (PFS) showed the decrease of randomness at the solid/solution interface in the biosorption system. For SPFS, ΔS° values are positive suggested the increased randomness at solid/solution interface during MG biosorption (Wojciech et al., 2018).

3.6. Biosorption isotherms

The biosorption isotherms analysis using the PFS and SPFS for the removal of MG carried out. The isotherm models constants values and respective coefficient of determination (R^2) are mentioned in Table 2. Fig. 1a–e illustrates the relative fit of biosorption isotherms studies with the biosorption experimental data. The coefficient of determination values of 0.995 (PFS) and 0.986 (SPFS) showed a strong positive evidence on the MG biosorption process follows the Langmuir isotherm model. The better fitted equilibrium data with linear form of the Langmuir model indicated in Fig. 1a. The well-fitted Langmuir isotherm model to the equilibrium data showed that MG biosorbed as a monolayer on PFS and SPFS at maximum biosorption capacity of 40.00 mg/g and 62.50 mg/g, respectively. The higher value of Langmuir constant (K_L), 0.3636 L/mg (SPFS) reveals the biosorption energy is higher for the binding of MG onto SPFS than PFS. The results point out the presence of stronger bonds between SPFS and MG and demonstrate chemisorption as the predominant mechanism of the biosorption process. The value of Freundlich constant (n) for PFS and SPFS towards MG biosorption found greater than, illustrates that MG favorably biosorbed onto biosorbent with stronger biosorption intensity. The R^2 values of 0.985 (PFS) and 0.978 (SPFS) was found for the Freundlich model fit to the biosorption equilibrium data, comparatively lower than Langmuir isotherm.

The values of the Tempkin isotherm model constants b_T and A_T are indicated in Table 2. The high R^2 values of 0.991 (PFS) and 0.988 (SPFS), implies that the heat of biosorption of all the MG dye molecules decreases with increasing coverage. The multilayer biosorption of dyes generally explained using Halsey isotherm model. Halsey isotherm model fitted the experimental data with R^2 values of 0.985 (PFS) and 0.978 (SPFS). The low values of K_H, 0.0090 (PFS) and 0.0014 (SPFS) suggested the less contribution of multilayer biosorption in the MG removal process. The Jovanovic isotherm demonstrates as one more approximation for monolayer coverage without any side interactions. The linear fit of experimental data with the Jovanovic isotherm model was presented in Fig. 1e. The maximum biosorption capacity predicted according to the Jovanovic model (Table 2) for MB removal found lesser compared to that of the Langmuir model calculated maximum uptake capacity. In comparison of the five isotherm models considered in the present study, the model of Langmuir, Tempkin are the better fitted biosorption isotherms and Jovanovic isotherm model, least fitted the equilibrium data of MG biosorption using PFS and SPFS.

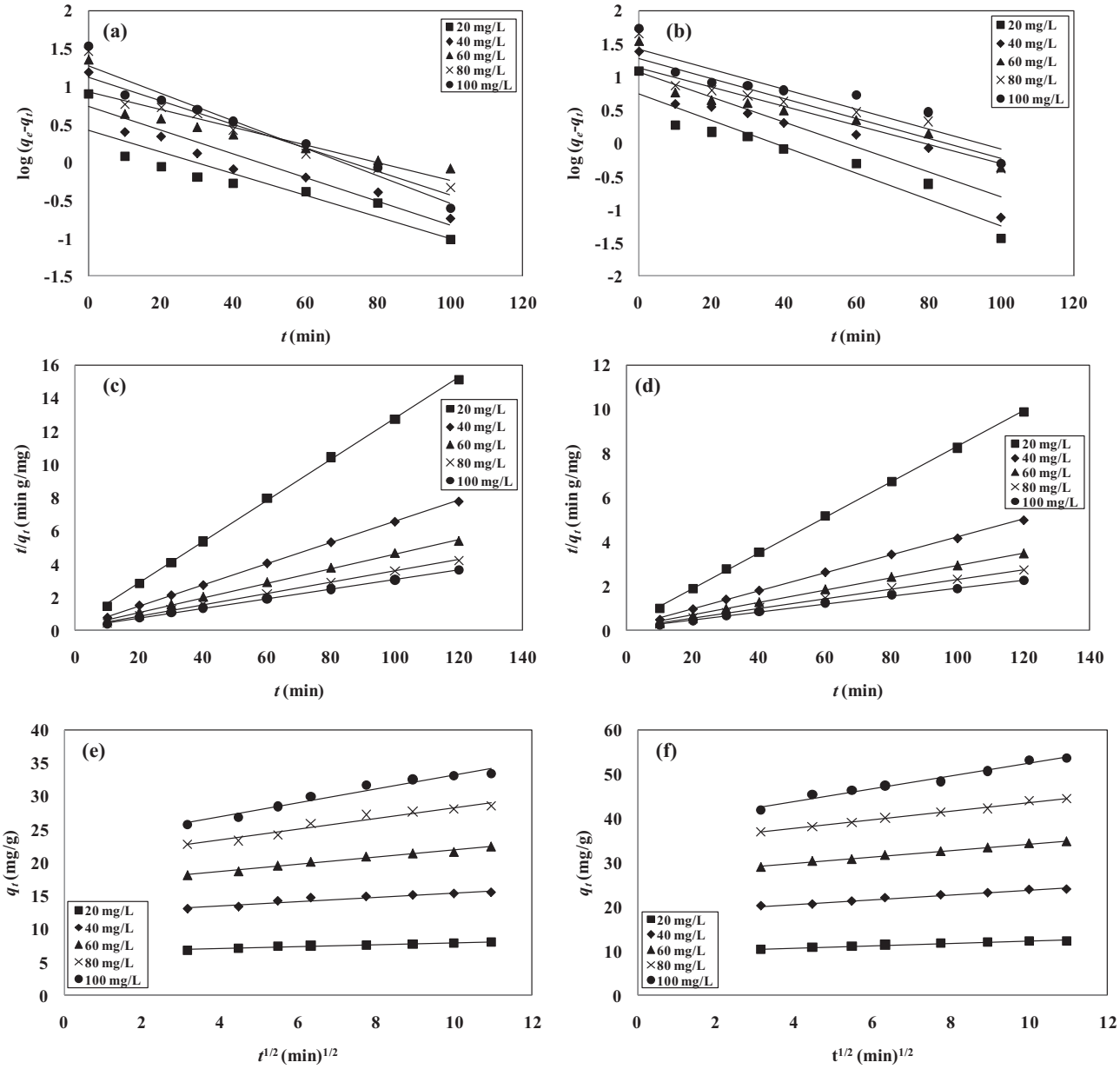

Fig. 2. Kinetic plots of (a) pseudo-first-order (PFS), (b) pseudo-first-order (SPFS), (c) pseudo-second-order (PFS), (d) pseudo-second-order (SPFS), (e) intra-particle diffusion (PFS) and (f) intra-particle diffusion (SPFS) kinetic models, for MG biosorption.

3.7. Biosorption kinetics

The predictions of the biosorption kinetic parameters are vital in the design of biosorption system. The parameters of the pseudo-first-order, pseudo-second-order and intra-particle diffusion kinetic models together with R^2 at different initial MG concentrations are summarized in Table 3.

From Fig. 2a, b and Table 3, the lower values of R^2 for all the initial MG concentrations, represent that the pseudo-first-order kinetic model failed to describe the MG kinetics using PFS and SPFS. The pseudo-second-order kinetic model better explains the experimental data over the entire contact time for PFS (Fig. 2c) and SPFS (Fig. 2d). The better fit of the pseudo-second-order kinetic model reveals that chemisorption involving valence force occurred through sharing or electron exchange between PFS, SPFS and MG is the rate controlling step (Zohra et al., 2011). The intra-particle diffusion model plots for the MG biosorption using PFS and SPFS are presented in Fig. 2e and f. According to the results of the plots obtained, the initial stage corresponds to the MG diffusion from the solution to the biosorbent external surface. The second stage denotes the gradual biosorption, representing intra-particle diffusion the rate controlling step. The third and final stage refers to the surface biosorption and the equilibrium attainment (Suyog and Parag, 2018). The R^2 values of intra-particle diffusion model for PFS and SPFS revealed that intra-particle diffusion model not the only rate determining step, associated with that further additional mechanisms participated in the biosorption of MG.

4. Conclusion

The fruit shells of *Peltophorum pterocarpum* evaluated in the native and modified form as potential biosorbents for MG removal from aqueous medium. Biosorption process parameters were found to affect the biosorption performance of MG using PFS and SPFS. The maximum biosorption capacities were 40.00 mg/g (PFS) and 62.50 mg/g (SPFS) for MG removal from aqueous medium. The better fitness of equilibrium data with Langmuir isotherm model recommended that MG

biosorption onto PFS and SPFS occurs through the monolayer formation. The kinetic analysis of the biosorption experimental data showed that the MG removal process fitted the pseudo-second-order kinetic model, illustrated chemisorption. The outcome of thermodynamic analysis of MG biosorption using SPFS, showed spontaneous and endothermic nature of removal process. Whereas, exothermic for MG biosorption by PFS. These results showed that fruit shells of *Peltophorum pterocarpum* in the native, NaOH pre-treated forms might be used as an effective biosorbent for treatment of water contaminated with malachite green.

Acknowledgments

The authors gratefully acknowledge the SASTRA University and National Institute of Technology Rourkela for providing the research facility.

References

Aida, K., Asma, M., Ghada, B.A., Mongi, S., 2016. Biosorption of alpacide blue from aqueous solution by lignocellulosic biomass: *Luffa cylindrica* fibers. Environ. Sci. Pollut. Res. 23, 15832–15840.

Anna, W.K., 2011. Analysis of influence of process conditions on kinetics of malachite green biosorption onto beech sawdust. Chem. Eng. J. 171, 976–985.

Baruah, S., Devi, A., Bhattacharyya, K.G., Sarma, A., 2017. Developing a biosorbent from *Aegle marmelos* leaves for removal of methylene blue from water. Int. J. Environ. Sci. Technol. 14, 341–352.

Binod, K., Upendra, K., 2015. Adsorption of malachite green in aqueous solution onto sodium carbonate treated rice husk. Korean J. Chem. Eng. 32, 1655–1666.

Ebrahim, S., Hossein, Z.K., Mehrorang, G., Arash, A., Ramin, J., 2018. Isotherms and kinetic study of ultrasound-assisted adsorption of malachite green and Pb^{2+} ions from aqueous samples by copper sulfide nanorods loaded on activated carbon: experimental design optimization. Ultrason. Sonochem. 40, 373–382.

Farnaz, H., Reza, N., Farimah, S., Hadi, S., 2016. Malachite green removal using modified sphagnum peat moss as a low-cost biosorbent: kinetic, equilibrium and thermodynamic studies. J. Taiwan Inst. Chem. Eng. 58, 482–489.

Freundlich, H., Helle, W., 1939. On adsorption in solution. J. Am. Chem. Soc. 61, 2228–2230.

Halsey, G., 1948. Physical adsorption on nonuniform surfaces. J. Chem. Phys. 16, 931–937.

Hemant, S., Garima, C., Arinjay, K.J., Sharma, S.K., 2017. Adsorptive potential of agricultural wastes for removal of dyes from aqueous solutions. J. Environ. Chem. Eng. 5, 122–135.

Ho, Y.S., McKay, G., 1999. Pseudo-second order model for sorption processes. Process Biochem. 34, 451–465.

Ho, Y.S., Ng, J.C.Y., Mckay, G., 2000. Kinetics of pollutant sorption by biosorbents: review. Sep. Purif. Methods 29, 189–232.

Isis, P.A.F.S., Andre, L.C., Osvaldo, P., Vitor, C.A., 2017. Preparation of biosorbents from the Jatoba (*Hymenaea courbaril*) fruit shell for removal of Pb(II) and Cd(II) from aqueous solution. Environ. Monit. Assess. 189, 632.

Jain, S.N., Gogate, P.R., 2017. NaOH-treated dead leaves of *Ficus racemosa* as an efficient biosorbent for Acid Blue 25 removal. Int. J. Environ. Sci. Technol. 14, 531–542.

Jeminat, O.A., Jose, H.S., Zahangir, M.A., Aminul, H.M., Chan, C.M., 2016. Adsorption of methylene blue from aqueous solution using untreated and treated (*Metroxylon* spp.) waste adsorbent: equilibrium and kinetics studies. Int. J. Ind. Chem. 7, 333–345.

Jovanovic, D.S., 1969. Physical adsorption of gases I: isotherms formonolayer and multilayer adsorption. Colloid Polym. Sci. 235, 1203–1214.

Lagergren, S., 1898. About the theory of so-called adsorption of soluble substances. K. Svenska Vetenskapsakad Handl 24, 1–39.

Langmuir, I., 1918. The adsorption of gases on plane surfaces of glass, mica and platinum. J. Am. Chem. Soc. 40, 1361–1403.

Malvin, M., Vusumzi, E.P., Sekomeng, J.M., 2017. Biosorption of lead(II) by chemically modified *Mangifera indica* seed shells: adsorbent preparation, characterization and performance assessment. Process. Saf. Environ. Prot. 111, 40–51.

Mohd, A.A., Rasyidah, A., 2011. Removal of malachite green dye from aqueous solution using rambutan peel-based activated carbon: equilibrium, kinetic and thermodynamic studies. Chem. Eng. J. 171, 510–516.

Muhammad, N.Z., Iqra, A., Raziya, N., Shahida, M., Usman, A.R., Salah, U.D.K., 2015. Characterization of chemically modified biosorbents from rice bran for biosorption of Ni(II). J. Taiwan Inst. Chem. Eng. 46, 82–88.

Mustafa, T.Y., Tushar, K.S., Sharmeen, A., Ang, H.M., 2014. Dye and its removal from aqueous solution by adsorption: a review. Adv. Colloid Interf. Sci. 209, 172–184.

Piccirillo, C., Moreira, I.S., Novais, R.M., Fernandes, A.J.S., Pullar, R.C., Castro, P.M.L., 2017. Biphasic apatite-carbon materials derived from pyrolysed fish bones for effective adsorption of persistent pollutants and heavy metals. J. Environ. Chem. Eng. 5, 4884–4894.

Rangabhashiyam, S., Balasubramanian, P., 2018a. Biosorption of hexavalent chromium and malachite green from aqueous effluents, using *Cladophora* sp. Chem. Ecol. https://doi.org/10.1080/02757540.2018.1427232.

Rangabhashiyam, S., Balasubramanian, P., 2018b. Adsorption behaviors of hazardous methylene blue and hexavalent chromium on novel materials derived from *Pterospermum acerifolium* shells. J. Mol. Liq. 254.

Rangabhashiyam, S., Selvaraju, N., 2015. Evaluation of the biosorption potential of a novel *Caryota urens* inflorescence waste biomass for the removal of hexavalent chromium from aqueous solutions. J. Taiwan Inst. Chem. Eng. 47, 59–70.

Rangabhashiyam, S., Anu, N., Selvaraju, N., 2013. The significance of fungal laccase in textile dye degradation – a review. Res. J. Chem. Environ. 17, 88–95.

Rangabhashiyam, S., Anu, N., Selvaraju, N., 2014a. Equilibrium and kinetic modeling of chromium (VI) removal from aqueous solution by a novel biosorbent. Res. J. Chem. Environ. 18, 30–36.

Rangabhashiyam, S., Anu, N., Giri Nandagopal, M.S., Selvaraju, N., 2014b. Relevance of isotherm models in biosorption of pollutants by agricultural byproducts. J. Environ. Chem. Eng. 2, 398–414.

Rangabhashiyam, S., Suganya, E., Lity, A.V., Selvaraju, N., 2016. Equilibrium and kinetics studies of hexavalent chromium biosorption on a novel green macroalgae *Enteromorpha* sp. Res. Chem. Intermed. 42, 1275–1294.

Rangabhashiyam, S., Lata, Sujata, Balasubramanian, P., 2018. Biosorption characteristics of methylene blue and malachite green from simulated wastewater onto *Carica papaya* wood biosorbent. Surf. Interfaces. https://doi.org/10.1016/j.surfin.2017.09.011.

Suyog, N.J., Parag, R.G., 2018. Efficient removal of Acid Green 25 dye from wastewater using activated *Prunus dulcis* as biosorbent: batch and column studies. J. Environ. Manag. 210, 226–238.

Tapas, K.R., Naba, K.M., 2017. Biosorption of Congo Red from aqueous solution onto burned root of *Eichhornia crassipes* biomass. Appl Water Sci 7, 1841–1854.

Tempkin, M.J., Pyzhev, V., 1940. Kinetics of ammonia synthesis on promoted iron catalysts. Acta Physiochim. URSS 12, 217–222.

Weber, W.J., Morris, J.C., 1962. Advances inwater pollution research: removal of biologically resistant pollutants from waste waters by adsorption. In: Proceedings of International Conference on Water Pollution Symposium, vol. 2. Pergamon Press, Oxford, pp. 231–266.

Wojciech, K., Agnieszka, H., Walerian, A., Ewa, M., 2018. Adsorption of cationic dyes onto Fe@graphite core–shell magnetic nanocomposite: equilibrium, kinetics and thermodynamics. Chem. Eng. Res. Des. 129, 259–270.

Zohra, B., Mejdi, J., Meriem, B., Fatima, A., Gwenaelle, T., 2011. Biosorption of basic dye from aqueous solutions by Date Stones and Palm-Trees Waste: kinetic, equilibrium and thermodynamic studies. Desalination 271, 80–87.